24. van Dijk FS, Nikkels PG, den Hollander NS, Nesbitt IM, van Rijn RR, et al. (2011) Lethal/severe osteogenesis imperfecta in a large family: a novel homozygous *LEPRE1* mutation and bone histological findings. Pediatr Dev Pathol 14: 228–34.
25. Zhang ZL, Zhang H, Ke YH, Yue H, Xiao WJ, et al. (2011) The identification of novel mutations in *COL1A1*, *COL1A2*, and *LEPRE1* genes in Chinese patients with osteogenesis imperfecta. J Bone Miner Metab (in press).
26. del Rio L, Carrascosa A, Pons F, Gusinyé M, Yeste D, et al. (1994) Bone mineral density of the lumbar spine in white Mediterranean Spanish children and adolescents: changes related to age, sex, and puberty. Pediatr Res 35: 362–366.
27. Sönnichsen B, Füllekrug J, Nguyen VP, Diekmann W, Robinson DG, et al. (1994) Retention and retrieval: both mechanisms cooperate to maintain calreticulin in the endoplasmic reticulum. J Cell Sci 107: 2705–2717.
28. Ishikawa Y, Wirz J, Vranka J, Nagata K, Bächinger H (2009) Biochemical characterization of the prolyl 3-hydroxylase 1·cartilage-associated protein·cyclophilin B complex. J Biol Chem 284: 17641–17647.

A Genome-Wide Expression Profile of Adrenocortical Cells in Knockout Mice Lacking Steroidogenic Acute Regulatory Protein

Tomohiro Ishii, Toshikatsu Mitsui, Sadafumi Suzuki, Yumi Matsuzaki, and Tomonobu Hasegawa

Departments of Pediatrics and Physiology, School of Medicine, Keio University, Tokyo 160-8582, Japan

Steroidogenic acute regulatory protein (StAR) facilitates cholesterol transfer into the inner mitochondrial membrane in the acute phase of steroidogenesis. Mice lacking StAR ($Star^{-/-}$) share phenotypes with human individuals having congenital lipoid adrenal hyperplasia including compromised production of steroid hormones and florid accumulation of cholesterol esters in adrenal glands and gonads. To define a specific pattern of molecular changes with StAR deficiency, we performed transcriptome analysis of adrenal cells selectively isolated by fluorescent-activated cell sorting at embryonic d 17.5 or 18.5 in seven wild-type ($Star^{+/+}$) or four $Star^{-/-}$ mice having the transgene targeting the enhanced green fluorescent protein to cell lineages that express StAR. A gene expression profile was obtained by whole-mouse genome microarray and confirmed by quantitative real-time PCR, identifying 1206 and 767 significantly up-regulated and down-regulated genes, respectively, in $Star^{-/-}$ mice compared with $Star^{+/+}$ mice (fold difference ≥ 2 and P value < 0.05 with false discovery rate < 0.2). In $Star^{-/-}$ mice, expression levels of genes involved in cholesterol efflux and the inflammatory response were significantly up-regulated, whereas those related to steroid hormone biosynthesis or cholesterol biosynthesis and influx were not significantly changed. Immunoreactive Iba1 or F4/80 (macrophage marker) in adrenal glands of $Star^{-/-}$ mice was detected not only in an increased number of resident macrophages but also in most adrenocortical cells. These findings expand our understanding of the pathophysiology of adrenal glands with the disruption of StAR and propose a reciprocal interaction between adrenocortical cells and resident macrophages inside adrenal glands of $Star^{-/-}$ mice. **(*Endocrinology* 153: 2714–2723, 2012)**

Steroidogenic acute regulatory protein (StAR) is one of the mitochondrial proteins under complex transcriptional control that is localized at crista facing the inner mitochondrial membrane or at the intermembrane space in steroidogenic cells, based on immunohistochemistry and electron microscopy (1, 2). StAR functions on the cytoplasmic aspect of the outer mitochondrial membrane, facilitates translocation of cholesterol from the outer to the inner mitochondrial membrane when newly synthesized, and regulates the rate-limiting step of steroidogenesis (3–7). Both humans having *STAR* mutations [congenital lipoid adrenal hyperplasia (lipoid CAH)] and knockout mice lacking StAR ($Star^{-/-}$ mice) show significant defects in steroid hormone biosynthesis and diffuse accumulation of lipid droplets in the steroidogenic cells of the adrenal glands and gonads (8–11). It has been well described that the onset of steroid hormone deficiency is variable among the adrenal cortex, testis, and ovary, leading to a two-hit model for the pathogenesis of lipoid CAH (8). This model proposes that the ultimately accumulated cholesterol esters abrogate the residual capacity of the StAR-independent steroidogenesis that are initially preserved in StAR-deficient steroidogenic cells. However, the molecular mechanism behind the pathophysiology of steroidogenic cells in StAR deficiency remains to be clarified.

ISSN Print 0013-7227 ISSN Online 1945-7170
Printed in U.S.A.

doi: 10.1210/en.2011-1627 Received August 14, 2011. Accepted March 28, 2012.
First Published Online April 23, 2012

Abbreviations: BAC, Bacterial artificial chromosome; E, embryonic day; eGFP, enhanced green fluorescent protein; FAC, fluorescent-activated cell (sorting); IPA, Ingenuity Pathways Analysis; lipoid CAH, congenital lipoid adrenal hyperplasia; LXR, liver X receptor; Mc2r, melanocortin type 2 receptor; qPCR, quantitative real-time PCR; SF-1, steroidogenic factor-1; Shh, sonic hedgehog; StAR, steroidogenic acute regulatory protein; Tlr2, toll-like receptor-2; Wnt4, wingless-related mouse mammary tumor virus integration site 4.

To delineate the molecular mechanism of cholesterol transport by StAR into the inner mitochondrial membrane, we have previously performed *in vivo* studies using bacterial artificial chromosome (BAC) transgenesis (11). We targeted expression of either wild-type StAR or mutant StAR lacking its mitochondrial targeting signal in $Star^{-/-}$ mice, confirming the ability of StAR lacking the mitochondrial targeting signal to perform some essential functions but also demonstrating the important functional defects in adrenal glands and gonads (11). This observation still needs confirmation because it differs from previous *in vitro* studies (6, 12). Further to this, we created transgenic mice carrying a BAC transgene targeting enhanced green fluorescent protein (eGFP) to steroidogenic cells of the adrenal cortex and gonads under the control of all regulatory *cis* sequences of the *Star* gene (StAR/eGFP mice). The StAR/eGFP mice provided a useful strategy for selectively isolating steroidogenic cells that normally express StAR.

To define a specific pattern of global changes in gene expression with the disruption of StAR, we performed transcriptome analysis of putative steroidogenic cells in adrenal glands of $Star^{-/-}$ mice and deciphered gene ontogeny or biological pathways that could explain the pathophysiology of StAR deficiency. The present study identified significant changes of gene expression associated with cholesterol efflux and inflammatory response in adrenocortical cells, proposing the first evidence for a reciprocal interaction between adrenocortical cells and resident macrophages inside adrenal glands with disruption of StAR.

Materials and Methods

Experimental animals

All experiments involving mice were approved by the Laboratory Animals Center at School of Medicine, Keio University (Tokyo, Japan). We collected $Star^{+/+}$ or $Star^{-/-}$ embryos carrying the transgene expressing eGFP under the control of the endogenous *Star* regulatory sequences. As reported in our previous study (11), the transgene was created by insertion of eGFP cDNA into the coding region of *Star* in a bacterial artificial chromosome clone containing the *Star* gene with 47 kb of 5′- and 62 kb of 3′-flanking regions of the gene (StAR/eGFP BAC) and was proved to target eGFP reporter expression to steroidogenic cells in adrenal cortex, testis, and ovary of adult mice driven by *Star* endogenous promoter. Mice were genotyped by PCR assays using the primer sets detailed below. *Star* genotype was determined using a forward primer (ATGATGCACAGCCTTCCACGG), a reverse primer no. 1 (CCATCACTGGCAGAAGCTCAGA), and a reverse primer no. 2 (ATCTCGTCGTGACCCATGGC). Chromosomal sex was determined by the presence or absence of *Sry* gene using a forward primer (AAGCGCCCCATGAATGCATT) and a reverse primer (CGATGAGGCTGATATTTATA). The presence of the StAR-eGFP BAC transgene was examined using a forward primer (AGCTGAAGCCATATTGGGGAACAAG) and a reverse primer (AGTGAATTGTAATACGACTCACTATAGGGC). In compliance with ethical recommendations, all embryos were collected from pregnant female mice fully anesthetized with an intraabdominal injection of pentobarbital.

Cell sorting

We selectively purified steroidogenic cells from adrenal glands at embryonic day (E) 17.5 or 18.5 in $Star^{+/+}$ (n = 7) or $Star^{-/-}$ mice (n = 4) with the StAR/eGFP BAC transgene. Adrenal glands were dissected out from the embryos and single cell suspensions were prepared by enzymatic dissociation in PBS containing 0.125% trypsin, 0.5% EDTA, and 5% deoxyribonuclease I type IV (Sigma-Aldrich Corp., St. Louis, MO) for 30–60 min at 37 C with gentle shaking. Cells were spun down and resuspended in ice-cold PBS containing 3% fetal calf serum and passed through 40-μm cell strainers (Falcon BD Biosciences, Becton Dickinson, Franklin Lakes, NJ). eGFP-positive cells were selectively isolated by fluorescent-activated cell (FAC) sorting (Vantage SE; Becton Dickinson).

RNA preparation

Total RNA was isolated from FAC-sorted cell populations with TRIzol reagent (Invitrogen Corp., Carlsbad, CA) and the subsequent NucleoSpin RNA XS (Macherey-Nagel GmbH and Co. KG, Duren, Germany). RNA was quantified using a Nanodrop ND1000 spectrophotometer (Nanodrop Technologies, Wilmington, DE). RNA quality and integrity was assessed using an Agilent 2100 bioanalyzer (Agilent Technologies, Inc., Palo Alto, CA).

mRNA was linearly amplified from 1.0 ng total RNA from each mouse by MessageAmp II aRNA amplification kit (Applied Biosystems/Ambion, Austin, TX). In brief, double-stranded cDNA was synthesized with an oligo-dT primer bearing a T7 promoter using ArrayScript reverse transcriptase, and was used as a template for *in vitro* transcription with T7 RNA polymerase to generate multiple copies of amplified mRNA. Amplified mRNA was purified using an RNAeasy column (QIAGEN, Valencia, CA). 200 ng of mRNA was reverse transcribed to generate double-stranded cDNA templates for cRNA probes for microarray analysis by SuperScript II RT (Invitrogen Corp.) with oligodeoxythymidine primers.

Microarray analysis

The transcription profile was determined by microarray analysis with Cy3-labeled cRNA using one-color Quick Amp labeling kit (Agilent Technologies). Dye incorporation and cRNA yield was checked with a Nanodrop ND1000 spectrophotometer (Nanodrop Technologies). Cy3-labeled cRNA was hybridized to a whole-mouse genome microarray G4122F (Agilent Technologies). This array platform is comprised of 41,534 probes of 60-mer oligonucleotides, representing more than 41,000 transcripts of mouse genome (http://www.agilent.com). The hybridized chips were scanned with a gene array scanner (Agilent Technologies) at the Core Instrumentation Facility, School of Medicine, Keio University (Tokyo, Japan). The observed data were analyzed using Gene Spring GX 11.5.1 (Agilent Technologies). The raw expression values were normalized to

the 75th percentile in all samples, and the data from very low signal values (less than the 20th percentile) were removed. The difference in gene expression was assessed by averaging the normalized values and performing a pairwise analysis between $Star^{+/+}$ mice and $Star^{-/-}$ mice. Differentially expressed genes were defined as having a difference in a gene expression ratio of 2-fold or greater and a P value using a Student t test of less than 0.05 with a false discovery rate (Q value) of Benjamin and Hochberg (13) of less than 0.2, according to recommendations by the MicroArray Quality control (14, 15).

Furthermore, gene ontogeny and biological pathway analyses for the differentially expressed genes were performed through Ingenuity Pathways Analysis (IPA) version 9 (Ingenuity Systems, Inc., Redwood City, CA) and NextBio (https://www.nextbio.com, Cupertino, CA). The IPA revealed the canonical pathways most significantly relevant to the data set of the microarray analysis by right- or two-tailed Fisher's exact probability test. NextBio identified a list of biogroups or cell types most significantly correlated with the differentially expressed genes based on the information of available 967 RNA expression studies with 318 mouse cell types (as of October 22, 2011) (16). A correlation score represents magnitude of correlation between gene expression profiles, computed with the running Fisher algorithm, a nonparametric rank-based statistical approach. A P value was determined by Fisher's exact probability test with multiple comparison test.

Quantitative real-time PCR (qPCR)

The expression levels for genes of interest were validated by qPCR with additional samples of FAC-sorted cells from adrenal glands of $Star^{+/+}$ (n = 3) or $Star^{-/-}$ males (n = 4) at E17.5 or 18.5. Total RNA was isolated and mRNA was amplified by the same methods as the microarray analysis. Two hundred forty nanograms of mRNA were reverse transcribed using SuperScript II RT (Invitrogen) with oligo-deoxythymidine primers. qPCR reactions were performed in 10-μl volumes containing cDNA synthesized from 0.5 ng mRNA by the intercalater method using SYBR Premix Ex Taq II (Takara Bio Inc., Otsu, Japan) and ABI Prism 7500 Fast (PE Applied Biosystems, Foster City, CA). Primer pairs were purchased from Takara Bio Inc., except for primers for *Cyp11a1* (17). The reaction conditions were 3 min at 95 C and 40 cycles of 15 sec at 95 C and 1 min at 60 C. The relative quantity of gene expression was calculated using the delta delta cycle threshold method. The average dCt of $Star^{+/+}$ mice was determined as a calibrator. *Gapdh* was chosen as an endogenous control for normalization of each gene studied, based on a step-wise comparison method with other housekeeping genes including *Ras18*, *Ywhaz*, *Tbp*, and *Hprt1* (18). Amplification of specific transcripts was confirmed by melting curve profiles at the end of each PCR. qPCR data were analyzed using 7500 Software version 2.0 (PE Applied Biosystems). Statistical difference in gene expression levels between $Star^{+/+}$ and $Star^{-/-}$ mice was examined using a Student t test, with $P < 0.05$ considered significant. A comparison of the fold changes of gene expression level between the microarray and the qPCR was analyzed using the Bland-Altman method (19) (MedCalc Software, Mariakerke, Belgium), with $P < 0.05$ considered significant.

Immunohistochemistry

Immunohistochemical analysis was performed on frozen tissues for eGFP or on fixed whole embryos for macrophage markers or steroidogenic factor-1 (SF-1; Nr5a1). For eGFP analysis, adrenal glands or gonads were harvested from each embryo at E17.5 and 18.5, embedded in Tissue Tek (Sakura, Tokyo, Japan), and stored at −80 C. The cryosections of the adrenal glands and the gonads were fixed by 4% paraformaldehyde in PBS for 10 min at room temperature. For analysis of the macrophage markers and SF-1, whole embryos were directly fixed by Tissue Fixative (Genostaff Co., Ltd., Tokyo, Japan) for 2 d at room temperature. Embryo sections containing adrenal glands were treated with proteinase K. For both preparations, endogenous peroxidase was blocked with 0.3% hydrogen peroxide in methanol for 30 min, followed by incubation with protein block (Dako, Glostrup, Denmark) and avidin/biotin blocking kit (Vector laboratories, Burlingame, CA). The sections were incubated with either rabbit antigreen fluorescent protein polyclonal antibodies (Molecular Probes, Eugene, OR), monoclonal antibody against macrophages (F4/80 antigen) (Acris Antibodies GmbH, Herford, Germany), rabbit anti-Iba1 polyclonal antibodies (Wako Pure Chemical Industries, Ltd., Osaka, Japan), or monoclonal antibody against SF-1 (TransGenic, Inc., Kobe, Japan) at 4 C overnight. After washing with Tris-buffered saline, they were incubated with biotin-conjugated immunoglobulin for 30 min at room temperature, followed by the addition of peroxidase-conjugated streptavidin (Nichirei Biosciences Inc., Tokyo, Japan) for 5 min. Peroxidase activity was visualized by diaminobenzidine. The sections were counterstained with Mayer's hematoxylin (Muto Pure Chemical Co., Ltd., Tokyo, Japan), dehydrated, and then mounted with Malinol (Muto).

Results

eGFP expression in adrenal glands of StAR/eGFP transgenic mice at E17.5 and 18.5

To isolate steroidogenic cells from adrenal glands, we used transgenic mice carrying the StAR/eGFP BAC transgene, which drives eGFP expression under control of the endogenous *Star* promoter. It has been reported that StAR is specifically expressed in steroidogenic cells such as adrenocortical cells, Leydig cells, theca cells, neurons, and glial cells (7). To confirm which cell lineages express eGFP within adrenal glands or testes, we examined intrinsic fluorescence of eGFP (data not shown) and immunoreactivity against eGFP antibodies with embryos carrying the StAR/eGFP BAC transgene at E17.5 and 18.5. As shown in Fig. 1, eGFP expression was identified in the adrenal cortex and in the interstitial region of the testis in $Star^{+/+}$ or $Star^{-/-}$ mice having the transgene, consistent with the location of adrenocortical and Leydig cells. No eGFP expression was determined in the fetal ovaries. At this developmental stage, eGFP expression was comparable in the adrenal cortex of male and female embryos. Overall, the StAR/eGFP BAC transgene targets eGFP to endoge-

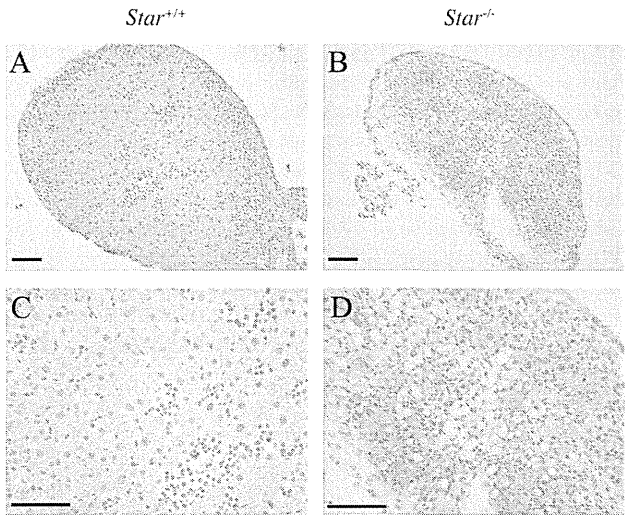

FIG. 1. Expression of Star/eGFP BAC transgene in adrenal glands of $Star^{+/+}$ or $Star^{-/-}$ mice at E17.5–18.5 by immunohistochemistry. A and C, $Star^{+/+}$. B and D, $Star^{-/-}$. C and D show higher magnification of A and B, respectively. *Scale bars*, 100 μm.

nous steroidogenic cells in adrenal glands and testes at E17.5 and 18.5, as we previously reported in adult mice.

Microarray analysis

To define specific changes associated with StAR deficiency, we performed transcriptome analysis with sorted eGFP-positive cells in adrenal glands of $Star^{+/+}$ or $Star^{-/-}$ embryos and identified a total of 1973 differentially expressed genes between them (Supplemental Table 1 and 2 published on The Endocrine Society's Journals Online web site at http://endo.endojournals.org). All original microarray data described in this study were submitted on a public database, National Center for Biotechnology Information's Gene Expression Omnibus (http://www.ncbi.nlm.nih.gov/geo) and is accessible through Gene Expression Omnibus series accession number GSE31328. Of 1973 differentially expressed genes, 1206 and 767 genes were significantly up-regulated and down-regulated, respectively, in adrenal steroidogenic cells derived from $Star^{-/-}$ mice compared with those from $Star^{+/+}$ mice (Supplemental Tables 1 and 2). No significant difference was found in expression of genes related to steroid hormone biosynthesis or cholesterol biosynthesis and influx, except for StAR. In contrast, genes related to cholesterol efflux such as those for liver X receptors (LXR) and ATP-binding cassettes were significant up-regulated. Adrenal glands at this stage also contain two different cell lineages, an adult zone in the outer cortices and a fetal zone in the inner cortices (20, 21). We found a significant decrease in expression of genes involved in the development of adrenocortical progenitor cells.

We performed further gene ontology and biological pathway analysis of the 1973 differentially expressed genes by using the IPA and the Nextbio and revealed the canonical pathways and biological functions to which differentially expressed genes were most significantly relevant. The IPA analysis unexpectedly revealed a significant association between the differentially expressed genes and the canonical pathways of inflammatory or immune response including dendritic cell maturation ($P = 2.1 \times 10^{-10}$), the antigen presentation pathway (1.4×10^{-9}), allograft rejection signaling (1.6×10^{-8}), the communication between innate and adaptive immune cells (1.0×10^{-7}), and IL-4 signaling (2.0×10^{-6}). Consistent with these data, the NextBio identified the immune response (correlation score 132.50, $P = 2.9 \times 10^{-58}$) as the most significant biogroup and the macrophage of the peripheral tissue of C57BL/6 (263.9, 2.5×10^{-115}), the microglial cell of C57BL/6 (255.8, 7.8×10^{-112}), and the dendritic cell follicular of lymph node of BALB/cAnNCrlCrlj (239.0, $1.6.8 \times 10^{-104}$) as the most significant cell types positively correlated with the differentially expressed genes. In fact, the genes related to the inflammatory or immune response were significantly up-regulated in the $Star^{-/-}$ mice.

Quantitative PCR

To verify the results of the microarray analysis, we determined gene expression levels of different samples by qPCR. We focused on genes of interest related to differentiation of adrenal glands, steroidogenesis, or cholesterol trafficking. The Bland-Altman plot analysis showed no statistically significant difference in fold changes of expression level of those genes between the microarray and the qPCR ($P = 0.245$) and no significant correlation between the difference and the average of fold changes for these factors ($r = 0.27$, $P = 0.05$), suggesting agreement of the fold changes between them. Consistent with the data from microarray analysis, the qPCR demonstrated significant up-regulation in genes related to cholesterol efflux, significant down-regulation in those involved in development of adrenocortical progenitor cells, and no significant change in those associated with steroid hormone biosynthesis or cholesterol biosynthesis and influx (Table 1).

Iba1 (Afi1) and F4/80 (Emr1) expressions in adrenal glands

We examined an expression pattern of macrophage-specific genes in the adrenal glands by immunohistochemistry at E17.5–18.5 with polyclonal antibodies against Iba1 or monoclonal antibody against F4/80 antigen. Iba1 and F4/80 are both specific markers for macrophages (22,

TABLE 1. Fold change in expression level of genes in knockout mice lacking StAR compared with those in wild-type mice by quantitative real-time PCR

Gene symbol	Description	Fold change (mean ± SE)
Steroid hormone biosynthesis		
Nr5a1	Nuclear receptor subfamily 5, group A, member 1	0.68 ± 0.52
Mc2r	Melanocortin 2 receptor	0.29 ± 0.18
Mrap	Melanocortin 2 receptor accessory protein	0.26 ± 0.51
Star	Steroidogenic acute regulatory protein	0.02 ± 0.01[a]
Cyp11a1	Cytochrome P450, family 11, subfamily a, polypeptide 1	0.63 ± 0.48
Fdx1	Ferredoxin 1	0.63 ± 0.69
Fdxr	Ferredoxin reductase	0.69 ± 0.56
Hsd3b1	Hydroxy-δ-5-steroid dehydrogenase, 3 β- and steroid δ-isomerase 1	0.51 ± 0.53
Agtr1a	Angiotensin II receptor, type 1a	0.76 ± 0.58
Cholesterol biosynthesis and influx		
Ldlr	Low-density lipoprotein receptor	1.58 ± 1.19
Scarb1	Scavenger receptor class B, member 1	1.39 ± 2.91
Hmgcr	3-Hydroxy-3-methylglutaryl-Coenzyme A reductase	0.77 ± 0.31
Lipe	Lipase, hormone sensitive	0.93 ± 0.45
Npc2	Niemann pick type C2	3.46 ± 4.7
Stard3	START domain containing 3	4.69 ± 3.15[a]
Bzrpl1	Benzodiazapine receptor, peripheral-like 1	0.82 ± 0.94
Srebf1	Sterol regulatory element binding factor 1	1.9 ± 0.93
Acat2	Acetyl-coenzyme A acetyltransferase 2	1.19 ± 1.08
Cholesterol metabolism and efflux		
Nr1h2	Nuclear receptor subfamily 1, group H, member 2	3.04 ± 1.21[a]
Nr1h3	Nuclear receptor subfamily 1, group H, member 3	7.76 ± 1.38[a]
Abca1	ATP-binding cassette, subfamily A (ABC1), member 1	2.92 ± 1.59[a]
Abcg1	ATP-binding cassette, subfamily G (WHITE), member 1	5.69 ± 3.1[a]
Abcb1a	ATP-binding cassette, subfamily B (MDR/TAP), member 1A	0.37 ± 0.93
Dhcr24	24-Dehydrocholesterol reductase	0.54 ± 0.62
ch25 h	Cholesterol 25-hydroxylase	0.57 ± 1.69
Adrenocortical development		
Wt1	Wilms tumor homolog	1.83 ± 1.26
Nr0b1	Nuclear receptor subfamily 0, group B, member 1	0.09 ± 0.10[a]
Shh	Sonic hedgehog	0.02 ± 0.02[a]
Wnt4	Wingless-related mouse mammary tumor virus integration site 4	0.08 ± 0.06[a]
Inflammatory response		
Cd86	CD86 antigen	6.44 ± 3.39[a]
Cd36	CD36 antigen	3.29 ± 2.03[a]
Cd5l	CD5 antigen-like	130.95 ± 273.32[a]
Spp1	Secreted phosphoprotein 1	259.15 ± 133.85[a]
Ccl5	Chemokine (C-C motif) ligand 5	113.14 ± 144.27[a]
Cxcl9	Chemokine (C-X-C motif) ligand 9	0.28 ± 1.23
Clec7a	C-type lectin domain family 7, member a	100.69 ± 65.1[a]
H2-Aa	Histocompatibility 2, class II antigen A, α	36.41 ± 147.76
H2-Ab1	Histocompatibility 2, class II antigen A, β1	24.29 ± 70.12
H2-Ea	Histocompatibility 2, class II antigen Eα	37.09 ± 475.29
Tlr1	Toll-like receptor 1	4.12 ± 3.97
Tlr2	Toll-like receptor 2	2.82 ± 2.31
Tlr4	Toll-like receptor 4	2.08 ± 1.24
Tlr6	Toll-like receptor 6	8.2 ± 8.33
Tlr7	Toll-like receptor 7	4.59 ± 3.41

[a] Statistically significant change ($P < 0.05$).

23). As shown in Fig. 2, Iba1 or F4/80 immunoreactivity was identified in only a few SF-1-negative resident macrophages within the adrenal cortex of $Star^{+/+}$ mice. By contrast, in the adrenal cortex of $Star^{-/-}$ mice, immunoreactivity was detected not only in an increased number of SF-1-negative resident macrophages but also for most adrenocortical cells.

Discussion

In this study, we performed transcriptome analysis of eGFP-positive cells selectively purified from adrenal glands in $Star^{-/-}$ mice carrying the StAR/eGFP BAC transgene. StAR regulates the acute phase of steroidogenesis and is expressed throughout the adrenal cortex at E12.5

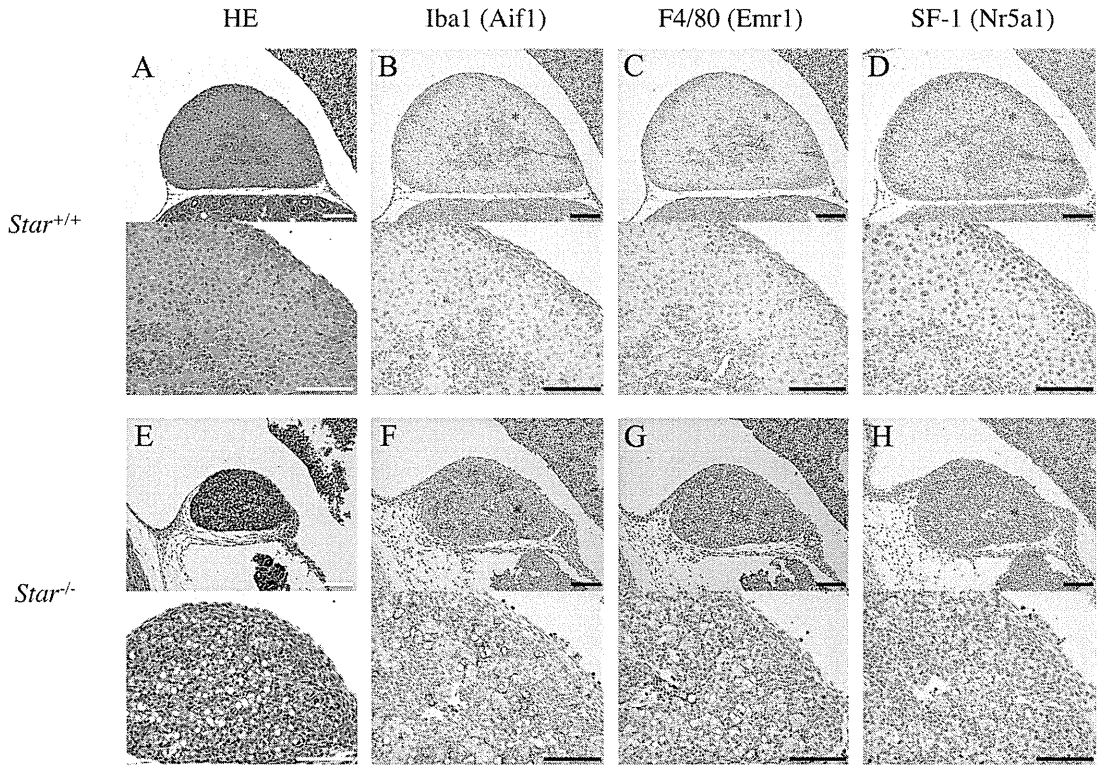

FIG. 2. Expression of macrophage markers in adrenal glands of $Star^{+/+}$ or $Star^{-/-}$ mice at E17.5–18.5 by immunohistochemistry. A–D, $Star^{+/+}$. E–H, $Star^{-/-}$. The *lower panels* show higher magnification of the area around the *asterisk* in the *upper panels*. *Scale bars*, 100 μm.

and later. Indeed, eGFP expression at E17.5 and E18.5 was consistent with endogenous StAR expression in adrenocortical cells as well as fetal Leydig cells. Thus, our experimental data showing 1973 differentially expressed genes convincingly identify the molecular characteristics specific for adrenocortical cells of $Star^{-/-}$ mice.

To clarify the two-hit model for lipoid CAH, we first focused on an expression profile of genes related to cholesterol biosynthesis and influx and steroid hormone biosynthesis. No significant difference was found in the expression of those pathways between the genotypes. ACTH levels of the newborn $Star^{-/-}$ mice were significantly higher than those of the newborn $Star^{+/+}$ mice (Sasaki G., unpublished data). Thus, the up-regulation of signal transduction for melanocortin type 2 receptor (Mc2r) was suppressed in $Star^{-/-}$ mice. This notion is consistent with adrenocortical quiescence that was described as a period of decreased responsiveness to ACTH in the midgestation of fetal sheep (24). In fact, the growth rate of fetal rat adrenal glands actually decreased as term approached (25). By contrast, genes related to cholesterol mobilization and efflux were significantly up-regulated in $Star^{-/-}$ mice. Therefore, although adrenocortical quiescence may be the case, it is inferred that the $Star^{-/-}$ mice-derived adrenocortical cells coordinate the pathways for cholesterol distribution to prevent malfunction due to the accumulation of free cholesterol.

Cummins (26) demonstrated that LXRα and -β (*Nr1h3* and *Nr1h2*, respectively) possessed a pivotal role in preventing the accumulation of free cholesterol in adrenal glands because knockout mice lacking LXRα and -β ($Lxr\alpha\beta^{-/-}$ mice) exhibited cholesterol ester accumulation. Consistent with this notion, the present study revealed the significant up-regulation of LXRα and -β in the adrenocortical cells of $Star^{-/-}$ mice that were full of cholesterol esters in the cytosol. The LXR up-regulation could result from the accumulation of oxysterol intermediates that work as ligands for LXR within the adrenocortical cells of $Star^{-/-}$ mice and lead to an induction of cholesterol efflux by increased expression of ATP-binding cassettes (*Abca1* and *Abcg1*). Furthermore, the increased LXR signaling could inhibit the expression of multiple steroidogenic genes as reported in the H295R human adrenocortical cell line (27). $Lxr\alpha\beta^{-/-}$ mice showed an increased adrenal steroidogenesis, even with a slight increase in StAR expression, indicating the possible link between repression of LXR signaling and increase in StAR-independent steroidogenesis. These findings give additional credence to the

role of LXR in the basal maintenance of adrenal cholesterol homeostasis and also imply the relevance of LXR up-regulation to the loss of residual capacity of StAR-independent steroidogenesis as the second hit of the two-hit model for lipoid CAH.

This study highlights another pathophysiological process likely modulated by StAR deficiency. We found that genes involved in the inflammatory or immune response showed significant positive correlation with the differentially expressed genes in *Star*$^{-/-}$ mice-derived adrenocortical cells. In addition, we identified significantly higher mRNA levels of the epithelial growth factor-like module containing, mucin-like, hormone receptor-like sequence 1 (*Emr1*) and integrin-αX (*Itgax*), markers for total and M1 , respectively. We also confirmed Iba1 or F4/80 (Emr1) immunoreactivity in the adrenal cortex of *Star*$^{-/-}$ mice, suggesting that adrenal steroidogenic cells express certain inflammatory response markers such as macrophages. It may be possible that the cytokine signaling of macrophages modifies the expression or function of molecules involved in steroidogenesis. Woods and Judd (28) previously described that IL-4 signaling inhibited the expression of steroidogenic enzymes induced by ACTH in bovine zona reticularis cells. IL-4 is one of the T-helper 2-type cytokines and is able to activate macrophages in an alternative fashion (29). In fact, IL-4 signaling was one of the canonical pathways in which the genes were significantly up-regulated in *Star*$^{-/-}$ mice. Therefore, the increased inflammatory or immune response, including IL-4 signaling, could be the second hit of the two-hit model for lipoid CAH, attenuating signal transduction of Mc2r under high levels of circulating ACTH.

The present findings also suggest a possible link between the inflammatory or immune system and adrenal glands. The adrenocortical cells produce a variety of cytokines during acute stress (30). The rat adrenal glands have been shown to contain resident macrophages (31, 32). The intraadrenal macrophages were reported to have a major role in affecting adrenal gland function in an autocrine or paracrine fashion (30). As shown in this study, *Star*$^{-/-}$ mice-derived adrenal glands contained a lot of macrophages. It could be possible that *Star*$^{-/-}$ mice-derived adrenocortical cells and resident macrophages interactively affect each other. In fact, *Star*$^{-/-}$ mice-derived adrenocortical cells exhibited significantly higher mRNA levels of chemokine ligand 5 (*Ccl5*) and CD36 antigen (*Cd36*). Chemokine ligand 5, one of the adipocytokines, recruits macrophages into adipose tissues (33). CD36, a receptor of apoptosis inhibitor of macrophage, induces lipolysis and chemokine production in adipocytes (34). These data suggest the adrenal glands in *Star*$^{-/-}$ mice share some of the characteristics of both adipocytes and macrophages in obesity-based chronic, low-grade inflammation of white adipose tissues (35–38), suggesting the possible reciprocal interaction between adrenocortical cells and macrophages in the pathological condition of cholesterol ester accumulation in the cytosol of adrenocortical cells.

The cytokine signals in adrenocortical cells may have a physiological role not only in the stress response but also in the maintenance of homeostasis, monitoring of malfunction, or adaptation to malfunction known as parainflammation (39). In fact, knockout mice lacking toll-like receptor-2 (Tlr2) demonstrated impaired corticosterone secretion at the basal or stress-induced stage and marked cellular disorganization in adrenal gland ultrastructure (40). Tlr2 signaling could be pivotal for sufficient amount of steroidogenesis in adrenal glands. Furthermore, the 3.5-kb StAR mRNA that is predominant in rodent steroidogenic cells contains five classical AU-rich elements in the 3′-untranslated region (41), which has been reported to stabilize mRNA in a number of cytokines involved in chronic inflammation (42). *Star* could share transcriptional regulation through the AU-rich elements with those cytokines. The actual role of parainflammation in adrenocortical cells still remains to be determined. Additional data are required to clarify the functional relevance of those cytokine signals to the physiological condition of adrenocortical cells.

It has recently been reported by the laboratory of Morohashi and colleagues (20, 21) that, by discovering a fetal adrenal-specific enhancer in the *Nr5a1* gene, the mouse adrenal cortex develops two distinct cell types, fetal and adult/definitive zones, during embryonic and early postnatal periods similar to human adrenal glands. The transition from fetal to adult adrenocortical cells was regulated by dosage-sensitive sex reversal-adrenal hypoplasia critical region on the X chromosome 1 (Nr0b1) and other growth factors expressed in the developing definitive zone, including the wingless-related mouse mammary tumor virus integration site 4 (Wnt4) and the sonic hedgehog (Shh) (21, 43–46). At E17.5 and E18.5, the definitive zone develops throughout the adrenal cortex, and the fetal zone remains at the inner part between the definitive zone and medulla. Most cells in the fetal and definitive zones express steroidogenic enzymes and possess the ability to produce steroid hormones at this stage. Thus, our expression profiles at E17.5–18.5 contained characteristics of both fetal and definitive zones. Interestingly, the components related to the transition of fetal to adult adrenocortical cells such as *Nr0b1*, *Wnt4*, and *Shh* were significantly down-regulated in *Star*$^{-/-}$ mice-derived adrenocortical cells. In fact,

the adrenal glands of *Star*$^{-/-}$ mice are hypoplastic in size and disorganized in cortical zonation. These data indicate that decreased expression of these components disturb proliferation and differentiation of the adrenal cortex in *Star*$^{-/-}$ mice.

We recognize the present study possesses potential limitations. First, the expression profile could be modified by excessive physical stress at the moment the animals were killed. We prudently used anesthesia for the pregnant female mice and quickly harvested the adrenal glands from the fetus to minimize physical stress. Second, the expression profile could be affected by the *in vitro* treatment of tissues with chemical digestion. We frequently watched tissues during digestion and ceased the reaction before they were damaged. Third, the expression profile could be biased by sex difference because our data were obtained from both female and male embryos. We did not identify any differentially expressed genes between male and female *Star*$^{+/+}$ embryos (Ishii T., unpublished observation). Finally, we would not rule out the possible recruitment of macrophages into an eGFP-positive cell population because autofluorescence or StAR expression was identified in the macrophages (47, 48). We set the adrenal glands of the *Star*$^{-/-}$ mice carrying no StAR/eGFP transgene as negative controls in FAC sorting. We did not find immunoreactive eGFP among Iba1-positive macrophages in the spleens of mice carrying the StAR/eGFP transgene at E17.5 and E18.5. It is less likely that macrophages in the adrenal cortex were sorted into eGFP-positive cells unless macrophages engulfed eGFP of adrenocortical cells. Given these caveats, the data presented conceivably reflect the pathological features in adrenocortical cells *in vivo* at E17.5–18.5.

In summary, we have demonstrated that StAR deficiency alters the gene expression profile of adrenocortical cells. This includes the significant up-regulation of genes associated with cholesterol efflux, especially LXR, preventing malfunction due to excessive accumulation of intracellular cholesterol, and the significant down-regulation of those regulating the development of adrenocortical zonation, leading to hypoplastic and disorganized structure of adrenal glands. This study also revealed a potentially pivotal role of the inflammatory or immune response in the pathological conditions of adrenocortical cells. This robust approach has expanded our understanding and helped to clarify the pathophysiology of steroidogenic cells with the disruption of StAR.

Acknowledgments

We sincerely dedicate this study to Dr. Keith L. Parker (Division of Endocrinology and Metabolism, Department of Internal Medicine, University of Texas Southwestern Medical Center, Dallas, TX), who passed away on December 12, 2008, after he kindly provided us with knockout mice lacking steroidogenic acute regulatory protein, in token of gratitude and appreciation for his generosity. We would like to thank Drs. Mie Hayashi, Naoko Amano, Masaki Takagi, and Ayuko Suwanai (Department of Pediatrics, School of Medicine, Keio University, Tokyo, Japan) for assistance, Drs. Satoshi Narumi (Department of Pediatrics, School of Medicine, Keio University, Tokyo, Japan), and Goro Sasaki (Department of Pediatrics, Tokyo Dental University, Ichikawa, Japan) for helpful discussion, Ms. Mari Fujiwara (the Core Instrumentation Facility, School of Medicine, Keio University, Tokyo, Japan) for microarray analysis, and Dr. Gareth Lavery (Centre for Endocrinology, Diabetes and Metabolism, Institute of Biomedical Research, University of Birmingham, Birmingham, UK) for reviewing the manuscript.

Address all correspondence and requests for reprints to: Tomohiro Ishii, M.D., Ph.D., Department of Pediatrics, School of Medicine, Keio University, 35 Shinanomachi, Shinjuku-ku, Tokyo 160-8582, Japan. E-mail: tishii@1992.jukuin.keio.ac.jp.

This work was supported by a Grant-in-Aid for Scientific Research (C) from the Japan Society for the Promotion of Science and a Research Grant from the Yamaguchi Endocrine Research Foundation.

Disclosure Summary: The authors have nothing to disclose.

References

1. **Cherradi N, Rossier MF, Vallotton MB, Timberg R, Friedberg I, Orly J, Wang XJ, Stocco DM, Capponi AM** 1997 Submitochondrial distribution of three key steroidogenic proteins (steroidogenic acute regulatory protein and cytochrome p450scc and 3β-hydroxysteroid dehydrogenase isomerase enzymes) upon stimulation by intracellular calcium in adrenal glomerulosa cells. J Biol Chem 272:7899–7907
2. **Stocco DM, Clark BJ, Reinhart AJ, Williams SC, Dyson M, Dassi B, Walsh LP, Manna PR, Wang XJ, Zeleznik AJ, Orly J** 2001 Elements involved in the regulation of the StAR gene. Mol Cell Endocrinol 177:55–59
3. **Stocco DM** 2001 StAR protein and the regulation of steroid hormone biosynthesis. Annu Rev Physiol 63:193–213
4. **Artemenko IP, Zhao D, Hales DB, Hales KH, Jefcoate CR** 2001 Mitochondrial processing of newly synthesized steroidogenic acute regulatory protein (StAR), but not total StAR, mediates cholesterol transfer to cytochrome P450 side chain cleavage enzyme in adrenal cells. J Biol Chem 276:46583–46596
5. **Jefcoate C** 2002 High-flux mitochondrial cholesterol trafficking, a specialized function of the adrenal cortex. J Clin Invest 110:881–890
6. **Bose HS, Lingappa VR, Miller WL** 2002 Rapid regulation of steroidogenesis by mitochondrial protein import. Nature 417:87–91
7. **Miller WL, Auchus RJ** 2011 The molecular biology, biochemistry, and physiology of human steroidogenesis and its disorders. Endocr Rev 32:81–151
8. **Bose HS, Sugawara T, Strauss 3rd JF, Miller WL** 1996 The pathophysiology and genetics of congenital lipoid adrenal hyperplasia. International Congenital Lipoid Adrenal Hyperplasia Consortium. N Engl J Med 335:1870–1878

9. **Hasegawa T, Zhao L, Caron KM, Majdic G, Suzuki T, Shizawa S, Sasano H, Parker KL** 2000 Developmental roles of the steroidogenic acute regulatory protein (StAR) as revealed by StAR knockout mice. Mol Endocrinol 14:1462–1471
10. **Ishii T, Hasegawa T, Pai CI, Yvgi-Ohana N, Timberg R, Zhao L, Majdic G, Chung BC, Orly J, Parker KL** 2002 The roles of circulating high-density lipoproteins and trophic hormones in the phenotype of knockout mice lacking the steroidogenic acute regulatory protein. Mol Endocrinol 16:2297–2309
11. **Sasaki G, Ishii T, Jeyasuria P, Jo Y, Bahat A, Orly J, Hasegawa T, Parker KL** 2008 Complex role of the mitochondrial targeting signal in the function of steroidogenic acute regulatory protein revealed by bacterial artificial chromosome transgenesis *in vivo*. Mol Endocrinol 22:951–964
12. **Arakane F, Kallen CB, Watari H, Foster JA, Sepuri NB, Pain D, Stayrook SE, Lewis M, Gerton GL, Strauss 3rd JF** 1998 The mechanism of action of steroidogenic acute regulatory protein (StAR). StAR acts on the outside of mitochondria to stimulate steroidogenesis. J Biol Chem 273:16339–16345
13. **Reiner A, Yekutieli D, Benjamini Y** 2003 Identifying differentially expressed genes using false discovery rate controlling procedures. Bioinformatics 19:368–375
14. **Shi L, Campbell G, Jones WD, Campagne F, Wen Z, Walker SJ, Su Z, Chu TM, Goodsaid FM, Pusztai L, Shaughnessy Jr JD, Oberthuer A, Thomas RS, Paules RS, Fielden M, Barlogie B, Chen W, Du P, Fischer M, Furlanello C, Gallas BD, Ge X, Megherbi DB, Symmans WF, Wang MD, *et al.*** 2010 The MicroArray Quality Control (MAQC)-II study of common practices for the development and validation of microarray-based predictive models. Nat Biotechnol 28:827–838
15. **Shi L, Reid LH, Jones WD, Shippy R, Warrington JA, Baker SC, Collins PJ, de Longueville F, Kawasaki ES, Lee KY, Luo Y, Sun YA, Willey JC, Setterquist RA, Fischer GM, Tong W, Dragan YP, Dix DJ, Frueh FW, Goodsaid FM, Herman D, Jensen RV, Johnson CD, Lobenhofer EK, Puri RK, *et al.*** 2006 The MicroArray Quality Control (MAQC) project shows inter- and intraplatform reproducibility of gene expression measurements. Nat Biotechnol 24:1151–1161
16. **Kupershmidt I, Su QJ, Grewal A, Sundaresh S, Halperin I, Flynn J, Shekar M, Wang H, Park J, Cui W, Wall GD, Wisotzkey R, Alag S, Akhtari S, Ronaghi M** 2010 Ontology-based meta-analysis of global collections of high-throughput public data. PLoS ONE 5:e13066
17. **Bouma GJ, Hart GT, Washburn LL, Recknagel AK, Eicher EM** 2004 Using real time RT-PCR analysis to determine multiple gene expression patterns during XX and XY mouse fetal gonad development. Gene Expr Patterns 5:141–149
18. **Vandesompele J, De Preter K, Pattyn F, Poppe B, Van Roy N, De Paepe A, Speleman F** 2002 Accurate normalization of real-time quantitative RT-PCR data by geometric averaging of multiple internal control genes. Genome Biol 3:RESEARCH0034-RESEARCH0034.0011
19. **Bland JM, Altman DG** 2003 Applying the right statistics: analyses of measurement studies. Ultrasound Obstet Gynecol 22:85–93
20. **Zubair M, Ishihara S, Oka S, Okumura K, Morohashi K-I** 2006 Two-step regulation of Ad4BP/SF-1 gene transcription during fetal adrenal development: initiation by a Hox-Pbx1-Prep1 complex and maintenance via autoregulation by Ad4BP/SF-1. Mol Cell Biol 26: 4111–4121
21. **Zubair M, Parker KL, Morohashi K-I** 2008 Developmental links between the fetal and adult zones of the adrenal cortex revealed by lineage tracing. Mol Cell Biol 28:7030–7040
22. **Kanazawa H, Ohsawa K, Sasaki Y, Kohsaka S, Imai Y** 2002 Macrophage/microglia-specific protein Iba1 enhances membrane ruffling and Rac activation via phospholipase C-γ-dependent pathway. J Biol Chem 277:20026–20032
23. **Lin HH, Stacey M, Stein-Streilein J, Gordon S** 2011 F4/80: the macrophage-specific adhesion-GPCR and its role in immunoregulation. Adv Exp Med Biol 706:149–156
24. **Boshier DP, Holloway H** 1989 Morphometric analyses of adrenal gland growth in fetal and neonatal sheep. I. The adrenal cortex. J Anat 167:1–14
25. **Bertholet JY** 1980 Proliferative activity and cell migration in the adrenal cortex of fetal and neonatal rats: an autoradiographic study. J Endocrinol 87:1–9
26. **Cummins CL, Volle DH, Zhang Y, McDonald JG, Sion B, Lefrançois-Martinez AM, Caira F, Veyssière G, Mangelsdorf DJ, Lobaccaro JM** 2006 Liver X receptors regulate adrenal cholesterol balance. J Clin Invest 116:1902–1912
27. **Nilsson M, Stulnig TM, Lin CY, Yeo AL, Nowotny P, Liu ET, Steffensen KR** 2007 Liver X receptors regulate adrenal steroidogenesis and hypothalamic-pituitary-adrenal feedback. Mol Endocrinol 21:126–137
28. **Woods AM, Judd AM** 2008 Interleukin-4 increases cortisol release and decreases adrenal androgen release from bovine adrenal cells. Domest Anim Endocrinol 34:372–382
29. **Gordon S, Martinez FO** 2010 Alternative activation of macrophages: mechanism and functions. Immunity 32:593–604
30. **Bornstein SR, Rutkowski H, Vrezas I** 2004 Cytokines and steroidogenesis. Mol Cell Endocrinol 215:135–141
31. **Sato T** 1998 Class II MHC-expressing cells in the rat adrenal gland defined by monoclonal antibodies. Histochem Cell Biol 109:359–367
32. **Schober A, Huber K, Fey J, Unsicker K** 1998 Distinct populations of macrophages in the adult rat adrenal gland: a subpopulation with neurotrophin-4-like immunoreactivity. Cell Tissue Res 291:365–373
33. **Keophiphath M, Rouault C, Divoux A, Clément K, Lacasa D** 2010 CCL5 promotes macrophage recruitment and survival in human adipose tissue. Arterioscler Thromb Vasc Biol 30:39–45
34. **Kurokawa J, Nagano H, Ohara O, Kubota N, Kadowaki T, Arai S, Miyazaki T** 2011 Apoptosis inhibitor of macrophage (AIM) is required for obesity-associated recruitment of inflammatory macrophages into adipose tissue. Proc Natl Acad Sci USA 108:12072–12077
35. **Gregor MF, Hotamisligil GS** 2011 Inflammatory mechanisms in obesity. Annu Rev Immunol 29:415–445
36. **Suganami T, Ogawa Y** 2010 Adipose tissue macrophages: their role in adipose tissue remodeling. J Leukoc Biol 88:33–39
37. **Trayhurn P, Wood IS** 2004 Adipokines: inflammation and the pleiotropic role of white adipose tissue. Br J Nutr 92:347–355
38. **Cottam DR, Mattar SG, Barinas-Mitchell E, Eid G, Kuller L, Kelley DE, Schauer PR** 2004 The chronic inflammatory hypothesis for the morbidity associated with morbid obesity: implications and effects of weight loss. Obes Surg 14:589–600
39. **Medzhitov R** 2008 Origin and physiological roles of inflammation. Nature 454:428–435
40. **Bornstein SR, Zacharowski P, Schumann RR, Barthel A, Tran N, Papewalis C, Rettori V, McCann SM, Schulze-Osthoff K, Scherbaum WA, Tarnow J, Zacharowski K** 2004 Impaired adrenal stress response in Toll-like receptor 2-deficient mice. Proc Natl Acad Sci USA 101:16695–16700
41. **Zhao D, Duan H, Kim YC, Jefcoate CR** 2005 Rodent StAR mRNA is substantially regulated by control of mRNA stability through sites in the 3′-untranslated region and through coupling to ongoing transcription. J Steroid Biochem Mol Biol 96:155–173
42. **Khabar KSA** 2010 Post-transcriptional control during chronic inflammation and cancer: a focus on AU-rich elements. Cell Mol Life Sci 67:2937–2955

43. **Kim AC, Barlaskar FM, Heaton JH, Else T, Kelly VR, Krill KT, Scheys JO, Simon DP, Trovato A, Yang WH, Hammer GD** 2009 In search of adrenocortical stem and progenitor cells. Endocr Rev 30: 241–263
44. **King P, Paul A, Laufer E** 2009 Shh signaling regulates adrenocortical development and identifies progenitors of steroidogenic lineages. Proc Natl Acad Sci USA 106:21185–21190
45. **Huang CC, Miyagawa S, Matsumaru D, Parker KL, Yao HH** 2010 Progenitor cell expansion and organ size of mouse adrenal is regulated by sonic hedgehog. Endocrinology 151:1119–1128
46. **Ching S, Vilain E** 2009 Targeted disruption of Sonic Hedgehog in the mouse adrenal leads to adrenocortical hypoplasia. Genesis 47:628–637
47. **Ma Y, Ren S, Pandak WM, Li X, Ning Y, Lu C, Zhao F, Yin L** 2007 The effects of inflammatory cytokines on steroidogenic acute regulatory protein expression in macrophages. Inflamm Res 56:495–501
48. **ten Hagen TL, van Vianen W, Bakker-Woudenberg IA** 1996 Isolation and characterization of murine Kupffer cells and splenic macrophages. J Immunol Methods 193:81–91

Tanaka et al. Experimental Hematology & Oncology 2012, 1:8
http://www.ehoonline.org/content/1/1/8

Experimental Hematology & Oncology

CASE REPORT Open Access

Hypoglycemia associated with L-asparaginase in acute lymphoblastic leukemia treatment: a case report

Ryuma Tanaka, Tomoo Osumi, Masashi Miharu, Tomohiro Ishii, Tomonobu Hasegawa, Takao Takahashi and Hiroyuki Shimada*

Abstract

A patient with acute lymphoblastic leukemia repeatedly developed hypoglycemia during chemotherapy. Comparison of serum glucose trends between chemotherapy with and without L-asparaginase (L-Asp) demonstrated a strong association between L-Asp and hypoglycemia. Critical blood sampling during hypoglycemia indicated hyperinsulinism, suggesting that L-Asp induced hypoglycemia in the patient through inappropriate insulin secretion. Identification of hypoglycemia as an adverse effect will enable clinicians to understand and develop appropriate strategies for L-Asp use in chemotherapy regimens.

Keywords: L-asparaginase, Fasting hypoglycemia, Hyperinsulinism, Acute lymphoblastic leukemia, Fasting Glucose levels

Background

The enzyme L-asparaginase (L-Asp) has been commonly used for treatment of childhood acute lymphoblastic leukemia (ALL) for more than 30 years [1-3]. Because of its unique pharmacological features and historically improved treatment outcomes, L-Asp forms an essential part of ALL regimens worldwide [4]. However, many adverse effects of L-Asp have been documented, such as coagulopathy, acute pancreatitis, allergic reaction, hyperlipidemia, hyperammonemia, hepatotoxicity, and hyperglycemia [5-8]. Therefore, clinicians must carefully monitor patients treated with L-Asp for these adverse effects. Until date, hypoglycemia has not been formally reported as an adverse effect of L-Asp. We report, for the first time, a case of hypoglycemia associated with L-Asp use.

Case presentation

A 5-year-old girl with Philadelphia chromosome-positive ALL was treated with the induction therapy protocol of the Tokyo Children's Cancer Study Group (TCCSG) L99-15 for high-risk patients. Therapy included prednisolone, vincristine, cyclophosphamide, daunorubicin, triple intrathecal injection, and L-Asp (Kyowa Hakko Kirin, Tokyo, Japan) [9]. The patient was administered 6000 IU/m^2 of native *Escherichia coli* L-Asp on days 16, 18, 20, 23, 25, 27, 30, 32, and 34 of treatment. On day 18, she developed fasting hypoglycemia (glucose, 56 mg/dL) with severe hunger and without other signs or symptoms such as tremor, palpitation, anxiety, sweating, or paresthesias. On day 27 (fasting serum glucose level, 50 mg/dL), critical blood sampling showed 6 U/mL of immunoreactive insulin, 0.47 mEq/L of free fatty acids, and 27 mol/L of ketone bodies. She repeatedly developed fasting hypoglycemia (glucose, 38–65 mg/dL) until day 37, without serious complications (Figure 1). Five days after the last L-Asp administration, her fasting glucose levels were elevated from 73 to 87 mg/dL. During induction therapy, fasting glucose levels were always measured before the morning steroid dose.

TCCSG L99-15 intensification-1, including high-dose cytarabine, methylprednisolone, L-Asp, and triple intrathecal injection, was started with daily imatinib. Thereafter, HR blocks of Berlin–Frankfurt–München (BFM) 2000 were administered. The HR blocks included cytarabine,

* Correspondence: hshimada@a5.keio.jp
Department of Pediatrics, Keio University School of Medicine, 35 Shinanomachi, Shinjuku-ku, Tokyo 160-8582, Japan

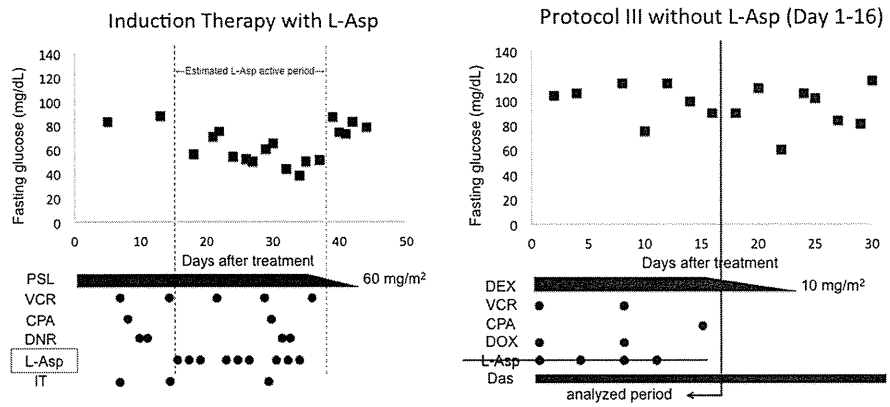

Figure 1 Fasting serum glucose levels during induction therapy with L-Asp and protocol III without L-Asp (Day 1–16). Monitoring of fasting serum glucose shows hypoglycemia during the estimated L-asp active period, displayed as the zone between dashed lines (----). PSL denotes predonisolone; VCR, vincristine; CPA, cyclophosphamide; DNR, daunorubicin; L-Asp, L-asparaginase; IT, intrathecal injection; DEX, dexamethasone; DOX, doxorubicin; and Das, dasatinib.

etoposide, methotrexate, vindesine, ifosfamide, daunorubicin, cyclophosphamide, dexamethasone, and L-Asp [10]. Daily dasatinib was included in the HR blocks instead of imatinib to avoid allergic reaction during TCCSG intensification-1. L-Asp was administered on day 5 of intensification-1 and days 6 and 11 of the HR block therapy. During early treatment days before L-Asp administration, the patient repeatedly developed fasting hyperglycemia (glucose, up to 132 mg/dL). After L-Asp administration, she repeatedly experienced fasting hypoglycemia and was provided with supplemental food and intravenous fluid containing dextrose to prevent severe hypoglycemia.

At the end of the third HR block, she suffered acute pancreatitis. When chemotherapy was resumed after 2 weeks of treatment for pancreatitis, L-Asp was excluded from protocol III of BFM 2000 (reinduction therapy), which included dexamethasone, vincristine, doxorubicin, cyclophosphamide, cytarabine, mercaptopurine, and intrathecal methotrexate administration. During protocol III, the patient did not experience hypoglycemia and had relatively high fasting glucose levels, up to 114 mg/dL (Figure 1).

Glucose levels during the estimated L-Asp active period were significantly lower than those before and after the induction therapy period (Student *t*-test, $p < 0.05$). The estimated L-Asp active period was defined as that from the first administration to 4 days after the last administration during induction therapy, given that the patient's fibrinogen level decreased with L-Asp and spontaneously recovered 5 days after the last L-Asp administration. This estimation is supported by a report that L-Asp activity is retained for 3 days in the BFM 2000 protocol, where 5000 IU/mL L-Asp is administered at 3-day intervals [11]. Thereafter, a linear regression model was used to identify the relationship between fasting glucose levels, L-Asp, and glucocorticoid potency during induction therapy and protocol III, with the same treatment structure as that of induction therapy. Variables were entered into a least-squares model. Prednisolone and dexamethasone potency was converted to hydrocortisone potency using 4:1 and 20:1 ratios, respectively [12]. Fasting glucose levels before and after the estimated L-Asp active period of induction therapy and during days 1–16 of protocol III were treated as values without L-Asp, whereas fasting glucose levels during the estimated L-Asp active period were treated as values with L-Asp. Linear regression analysis showed that fasting glucose levels were significantly lower during the L-Asp active period (42.91 mg/dL, $p < 0.001$), and the hyperglycemic effect of glucocorticoids was significant (glucose, 0.084 mg/dL per mg hydrocortisone equivalence, $p = 0.015$), indicating the following equation: glucose = 0.084 × [steroid potency] − 42.91 × [L-Asp use (1 or 0)] + 78.96 (Figure 2).

We confirmed that L-Asp activity was therapeutic during fasting hypoglycemia in the first HR block. L-Asp activity was 0.709 U/mL on day 10, 0.674 U/mL on day 11, and 1.78 U/mL on day 12, where 25000 U/m^2 of L-Asp was administered on days 6 and 11. L-Asp activity was measured using the enzyme coupling methods described by Tsurusawa et al. [13,14]. L-Asp activity above 0.1 U/mL was generally considered therapeutic. The detection limit of this method was 0.002 U/mL.

Conclusions

During ALL treatment, glucose levels are routinely monitored because many patients develop hyperglycemia, presumably because of glucocorticoids and L-Asp. Unexpectedly, our patient experienced repeated fasting

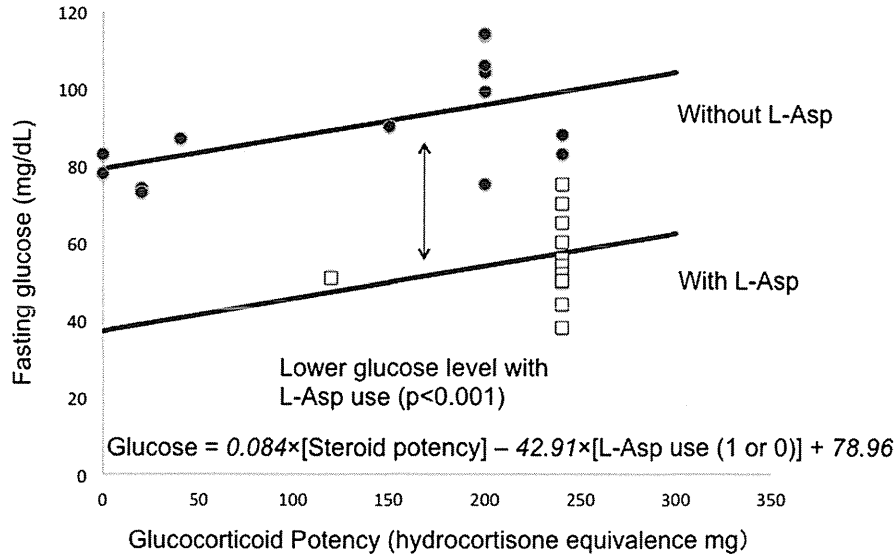

Figure 2 Linear regression analysis of fasting glucose, L-Asp, and glucocorticoid potency during induction therapy and protocol III. Linear regression analysis shows significant hypoglycemia during L-Asp use ($p < 0.001$) and a significant hyperglycemic effect of glucocorticoids ($p = 0.015$). Fasting glucose levels were plotted with L-Asp (□) and without L-Asp (●). Glucocorticoid potency is calculated as hydrocortisone equivalence with conversion ratios of 4:1 (prednisolone) and 20:1 (dexamethasone). L-Asp denotes L-asparaginase.

hypoglycemia during induction therapy, intensification-1, and HR block therapy. From induction through HR block therapy, L-Asp and steroids were both used and hypoglycemia was always observed after L-Asp use. Given the time relation between L-Asp administration and hypoglycemia, we hypothesized that our patient experienced L-Asp–induced hypoglycemia. Firstly, we compared fasting glucose levels with L-Asp and without L-Asp during induction (Student *T*-test), showing that those with L-Asp were significantly lower. After HR block therapy, L-Asp was excluded from protocol III because of the development of pancreatitis. Then, we compared fasting glucose levels during induction and first half of protocol III, the same backbone of treatment with and without L-Asp, respectively.

The following questions are to be answered: 1) How does L-Asp induce hypoglycemia? 2) Is there any use of other agents that might affect fasting glucose levels? 3) Why has hypoglycemia not been commonly seen or reported?

In response to the first question, inappropriate insulin secretion, normal free fatty acids, and low ketone bodies during severe hypoglycemia indicated hyperinsulinism, suggesting that L-Asp induced hypoglycemia through insulin hypersecretion. Regarding the second question, besides L-Asp use, there were the following differences between induction therapy and day 1–16 of protocol III; doxorubicin was used in protocol III instead of daunorubicin in induction therapy, and dasatinib was used in protocol III but not in induction therapy. Dasatinib has been not documented to cause the adverse effect of hyperglycemia or hypoglycemia. There was no use of other drugs that potentially induce hypoglycemia or hyperglycemia during these periods, such as non-steroidal anti-inflammatory drugs, antibacterial agents, or imatinib [15]. To the third question, there are few reports focusing on fasting glucose levels in the morning [6,7]. Glucocorticoids are known to induce hyperglycemia through insulin resistance and gluconeogenesis during induction therapy for childhood ALL [16]. We suspect that parallel use of glucocorticoids may mask the hypoglycemic effect of L-Asp. Since different glucocorticoid agents were used in these two regimens, we treated glucocorticoids as an independent parameter with glucocorticoid potency conversion. Linear regression model showed a significant L-Asp hypoglycemic effect as well as glucocorticoid hyperglycemic effect. There was no significant interaction between L-Asp and glucocorticoids. There remains a concern with validity of glucocorticoid potency conversion for hyperglycemic effect. To overcome the limitation of this case report, further clinical data focusing on hypoglycemia are needed.

Use of L-Asp has recently become even more common in the adult ALL regimens [17]. We believe that in addition to the effect of L-Asp on leukemic cells, it is important to pay more attention to its pharmacological features and physiological mechanisms. Greater knowledge of these effects will enable clinicians to

understand and develop appropriate strategies for L-Asp use in chemotherapy regimens.

Consent

Written informed consent was obtained from the patient's guardian for publication of this case report. A copy of the written consent is available for review by the Editor-in-Chief of this journal.

Abbreviations

L-Asp: L-asparaginase; ALL: Acute lymphoblastic leukemia; TCCSG: Tokyo Children's Cancer Study Group; BFM: Berlin–Frankfurt–München.

Competing interests

The authors declare that they have no competing interests.

Authors' contributions

RT designed and wrote the paper. TO, MM, and HS were responsible for the patient's overall treatment and review of the manuscript. TI and TH were responsible for the patient's endocrinological management and investigations. TT and HS performed their critical interpretation. All authors read and approved the final report.

Acknowledgments

We appreciate Mr. Haruki Honda for assisting in clinical data collection as a medical student.

Received: 18 March 2012 Accepted: 19 March 2012
Published: 19 April 2012

References

1. Möricke A, Zimmermann M, Reiter A, Henze G, Schrauder A, Gadner H, Ludwig WD, Ritter J, Harbott J, Mann G, Klingebiel T, Zintl F, Niemeyer C, Kremens B, Niggli F, Niethammer D, Welte K, Stanulla M, Odenwald E, Riehm H, Schrappe M: **Long-term results of five consecutive trials in childhood acute lymphoblastic leukemia performed by the ALL-BFM study group from 1981 to 2000.** *Leukemia* 2010, **24**:265–284.
2. Tsuchida M, Ohara A, Manabe A, Kumagai M, Shimada H, Kikuchi A, Mori T, Saito M, Akiyama M, Fukushima T, Koike K, Shiobara M, Ogawa C, Kanazawa T, Noguchi Y, Oota S, Okimoto Y, Yabe H, Kajiwara M, Tomizawa D, Ko K, Sugita K, Kaneko T, Maeda M, Inukai T, Goto H, Takahashi H, Isoyama K, Hayashi Y, Hosoya R, Hanada R, Tokyo Children's Cancer Study Group: **Long-term results of Tokyo Children's Cancer Study Group trials for childhood acute lymphoblastic leukemia, 1984–1999.** *Leukemia* 2010, **24**:383–396.
3. Gaynon PS, Angiolillo AL, Carroll WL, Nachman JB, Trigg ME, Sather HN, Hunger SP, Devidas M, Children's Oncology Group: **Long-term results of the children's cancer group studies for childhood acute lymphoblastic leukemia 1983–2002: a Children's Oncology Group Report.** *Leukemia* 2010, **24**:285–297.
4. Pession A, Valsecchi MG, Masera G, Kamps WA, Magyarosy E, Rizzari C, van Wering ER, Lo Nigro L, van der Does A, Locatelli F, Basso G, Aricò M: **Long-term results of a randomized trial on extended use of high dose L-asparaginase for standard risk childhood acute lymphoblastic leukemia.** *J Clin Oncol* 2005, **23**:7161–7167.
5. Raetz EA, Salzer WL: **Tolerability and efficacy of L-asparaginase therapy in pediatric patients with acute lymphoblastic leukemia.** *J Pediatr Hematol Oncol* 2010, **32**:554–563.
6. Pui CH, Burghen GA, Bowman WP, Aur RJ: **Risk factors for hyperglycemia in children with leukemia receiving L-asparaginase and prednisone.** *J Pediatr* 1981, **99**:46–50.
7. Carpentieri U, Balch MT: **Hyperglycemia associated with the therapeutic use of L-asparaginase: possible role of insulin receptors.** *J Pediatr* 1978, **93**:775–778.
8. Roberson JR, Raju S, Shelso J, Pui CH, Howard SC: **Diabetic ketoacidosis during therapy for pediatric acute lymphoblastic leukemia.** *Pediatr Blood Cancer* 2008, **50**:1207–1212.
9. Manabe A, Ohara A, Hasegawa D, Koh K, Saito T, Kiyokawa N, Kikuchi A, Takahashi H, Ikuta K, Hayashi Y, Hanada R, Tsuchida M: **Tokyo Children's Cancer Study Group: Significance of the complete clearance of peripheral blasts after 7 days of prednisolone treatment in children with acute lymphoblastic leukemia: the Tokyo Children's Cancer Study Group Study L99-15.** *Haematologica* 2008, **93**:1155–1160.
10. Conter V, Bartram CR, Valsecchi MG, Schrauder A, Panzer-Grümayer R, Möricke A, Aricò M, Zimmermann M, Mann G, De Rossi G, Stanulla M, Locatelli F, Basso G, Niggli F, Barisone E, Henze G, Ludwig WD, Haas OA, Cazzaniga G, Koehler R, Silvestri D, Bradtke J, Parasole R, Beier R, van Dongen JJ, Biondi A, Schrappe M: **Molecular response to treatment redefines all prognostic factors in children and adolescents with B-cell precursor acute lymphoblastic leukemia: results in 3184 patients of the AIEOP-BFM ALL 2000 study.** *Blood* 2010, **115**:3206–3214.
11. Schrey D, Borghorst S, Lanvers-Kaminsky C, Hempel G, Gerss J, Möricke A, Schrappe M, Boos J: **Therapeutic drug monitoring of asparaginase in the ALL-BFM 2000 protocol between 2000 and 2007.** *Pediatr Blood Cancer* 2010, **54**:952–958.
12. Meikle AW, Tyler FH: **Potency and duration of action of glucocorticoids. Effects of hydrocortisone, prednisone and dexamethasone on human pituitary-adrenal function.** *Am J Med* 1977, **63**:200–207.
13. Watanabe S, Miyake K, Ogawa C, Matsumoto H, Yoshida K, Hirabayashi S, Hasegawa D, Inoue T, Kizu J, Machida R, Ohara A, Hosoya R, Manabe A: **The ex vivo production of ammonia predicts L-asparaginase biological activity in children with acute lymphoblastic leukemia.** *Int J Hematol* 2009, **90**:347–352.
14. Tsurusawa M, Chin M, Iwai A, Nomura K, Maeba H, Taga T, Higa T, Kuno T, Hori T, Muto A, Yamagata M: **Japanese Children's Cancer and Leukemia Study Group: L-Asparagine depletion levels and L-asparaginase activity in plasma of children with acute lymphoblastic leukemia under asparaginase treatment.** *Cancer Chemother Pharmacol* 2004, **53**:204–208.
15. Ben Salem C, Fathallah N, Hmouda H, Bouraoui K: **Drug-induced hypoglycemia: an update.** *Drug Saf* 2011, **34**:21–45.
16. Lowas SR, Marks D, Malempati S: **Prevalence of transient hyperglycemia during induction chemotherapy for pediatric acute lymphoblastic leukemia.** *Pediatr Blood Cancer* 2009, **52**:814–818.
17. Hagop MK, Susan O, Terry LS, Cortes J, Giles FJ, Beran M, Pierce S, Huh Y, Andreeff M, Koller C, Ha CS, Keating MJ, Murphy S, Freireich EJ: **Results of Treatment With Hyper-CVAD, a Dose-Intensive Regimen, in Adult Acute Lymphocytic Leukemia.** *J Clin Oncol* 2000, **18**:547–561.

doi:10.1186/2162-3619-1-8
Cite this article as: Tanaka *et al.*: Hypoglycemia associated with L-asparaginase in acute lymphoblastic leukemia treatment: a case report. *Experimental Hematology & Oncology* 2012 1:8.

Endocrine Journal 2011, **58** (8), 647-655

ORIGINAL

High iFGF23 level despite hypophosphatemia is one of the clinical indicators to make diagnosis of XLH

Junko Miyamoto Igaki[1)], Makoto Yamada[1)], Yuji Yamazaki[2)], Shinobu Koto[1)], Masako Izawa[1)], Daisuke Ariyasu[1)], Eri Suzuki[1)], Hisashi Hasegawa[3)] and Yukihiro Hasegawa[1)]

[1)]*Division of Endocrinology and Metabolism, Tokyo Metropolitan Children's Hospital, Tokyo 183-8561, Japan*
[2)]*Antibody Research Laboratories, Kyowa Hakko Kirin Co., Ltd, Tokyo 194-8533, Japan*
[3)]*Innovative Drug Research Laboratories, Kyowa Hakko Kirin Co., Ltd, Tokyo 194-8533, Japan*

Abstract. X-linked hypophosphatemic rickets (XLH) is caused by inactivating mutations in the phosphate-regulating gene with homologies to endopeptidases on the X chromosome (PHEX) gene. Deletion of *Phex* leads to increased serum fibroblast growth factor23 (FGF23) levels in mouse. The aim is to assure the clinical usefulness of FGF23 determination in the diagnosis of XLH. Participants were 21 patients with XLH having abnormalities in *PHEX* from 13 kindred (PtPHEX: 1 to 42 years old; 10 males, 11 females) and 55 healthy controls (1 month to 18 years old; 27 males, 28 females). Temporal changes in FGF23 were determined by a single oral phosphate administration in PtPHEX and an ad lib diet in controls. Reference ranges of intact FGF23 (iFGF23) for children were determined. iFGF23 level which distinguish between controls and PtPHEX were validated. Correlations between iFGF23 and the severity of XLH (gender, age of onset, bone deformity, The ratio of maximum rate of renal tubular reabsorption of phosphate to glomerular filtration rate ($TmPO_4$/GFR), inorganic phosphate (IP), Alkaline Phosphatase (ALP), therapeutic dose) were investigated. Increasing tendency after phosphate administration and no general tendency after breakfast in iFGF23 were observed. Reference range (5^{th} and 95^{th} percentiles) of iFGF23 for children (12.9 and 51.2 pg/mL) was similar to that for adults. iFGF23 were above the reference range in 19 of 21 PtPHEX (40 to 4710 pg/mL). iFGF23 did not correlate with any index of severity of XLH. Relatively high iFGF23 despite hypophosphatemia is one of the clinical indicators to diagnose XLH.

Key words: X-linked hypophosphatemic rickets (XLH), FGF23, *PHEX* mutation, Reference range, Phosphate loading

FOUR genes responsible for hereditary hypophosphatemic rickets have been reported: X-linked hypophosphatemic rickets (XLH) caused by abnormalities in phosphate-regulating gene with homologies to endopeptidases on the X chromosome (PHEX) gene, autosomal dominant hypophosphatemic rickets (ADHR) caused by mutations in fibroblast growth factor23 (FGF23) gene [1], hypophosphatemic rickets with hypercalciuria caused by mutations in solute carrier family 34, member 3 (SLC34A3) gene, and autosomal recessive hypophosphatemic rickets caused by mutations in dentin matrix protein 1 (DMP1) [2, 3] or ectonucleotide pyrophosphatase/phosphodiesterase 1 (ENPP1) genes [4, 5]. The most common cause of hereditary hypophosphatemic rickets is XLH.

XLH is a disorder of mineralization of bone matrix caused by combined defects of phosphate reabsorption in the proximal tubule and calcitriol synthesis. Patients with XLH are treated with phosphate and vitamin D. More than 160 inactivating *PHEX* mutations are responsible for the clinical presentation of patients with XLH [6]. However, the mechanism whereby loss of PHEX function leads to the disease remains unknown. The current view is that, loss of PHEX function probably results in accumulation of phosphatonins which are circulating factors that regulate phosphate homeostasis and mineralization of bone. FGF23 [7], matrix extracellular phosphoglycoprotein (MEPE) [8], frizzled related protein 4 (FRP-4) [9] and FGF7 are the putative phosphatonins [10, 11].

FGF23 is a 32-kDa (251 amino acids) protein with an N-terminal region containing the FGF-homology

Received Sep. 2, 2010; Accepted May 6, 2011 as K10E-257
Released online in J-STAGE as advance publication May 19, 2011

Correspondence to: Junko M. Igaki, Division of Endocrinology and Metabolism, Tokyo Metropolitan Children's Hospital, 2-8-29, Musashidai, Fuchu-shi, Tokyo, 183-8561, Japan.
E-mail: junko_igaki@tmhp.jp

domain and a unique 71 amino acid C-terminus. It has been reported that full length FGF23 reduces serum phosphate and 1,25(OH)2D levels by reducing the renal sodium/inorganic phosphate co-transporter, type IIc (NaPi IIc) and type IIa (NaPi IIa) and by controlling renal expression of key enzymes of the vitamin D metabolism, respectively [12, 13].

FGF23 is central to the pathogenesis of XLH, for the following reasons: 1) the phenotype of patients with abnormalities in *PHEX* is similar to that of patients with abnormalities in *FGF23*[10], 2) serum FGF23 levels are high in the Hyp mouse [10], a model of XLH which harbors large deletions in the 3' region of the *Phex*, and 3) ablation of FGF23 in the Hyp mouse ameliorates the hypophosphatemic phenotype [7].

Serum FGF23 levels in patients with XLH are expected to be high since serum concentrations of FGF23 in Hyp mice are reported to be 10-fold higher when compared with normal mice [10]. Indeed, patients with XLH are reported to have high serum FGF23 levels [14-16]. However, diagnosis was not confirmed genetically in some patients. Serum FGF23 levels are also increased in patients with mutations in *FGF23*, *DMP1* and *ENPP1* called FGF23-related hypophosphatemic diseases [17]. It had been reported that low and high phosphate diet for more than 4 days reduces and increases FGF23 levels, respectively in both human [18-20]and mouse [21]. However, the short term effect of an oral phosphate load on FGF23 levels remains unknown. The clinical usefulness of FGF23 levels for the diagnosis of XLH with abnormalities in *PHEX* remains to be elucidated. The reference range of FGF23 levels for children has not been established, although that for adults is reported [14]. Whether FGF23 levels can predict disease severity also remains to be elucidated.

Objectives

The aims of the present study were the following: 1) to establish the temporal change in FGF23 levels in response to the short term administration of an oral phosphate load and diet, 2) to investigate the clinical usefulness of FGF23 determination in the diagnosis of XLH with abnormalities in *PHEX*. In order to investigate the second aim, we performed the following three sub studies: a) establish the reference range of FGF23 in the first two decades of life, b) validate the serum FGF23 levels which distinguish between healthy subjects and patients with abnormalities in *PHEX*, c) explore the correlation between the severity of XLH and FGF23 levels.

Participants

Patients with XLH bearing abnormalities in PHEX

Forty five patients (15 male, 30 female) with hypophosphatemic rickets from 35 kindred have been followed in our hospital from 1966 to 2007. Twenty-one of 45 patients (ages 1 to 42 years; 10 male, 11 female: 14 patients under 20 years old and 7 patients aged 20 years or over)) from 13 separate kindred who provided informed consent and were diagnosed as having abnormalities in *PHEX* were included in this study. Twenty-four patients were excluded from this study for the following reasons: 1) 22 patients had no gene analysis, 2) two patients had no abnormalities in *PHEX*. Among the 21 patients with abnormalities in *PHEX*, 20 patients were treated with 1-α hydroxyl vitamin D_3 (alfarol®) and phosphate at the time of the study, and one patient was not on medications. Treatment dosages of phosphate were adjusted individually to achieve an increase in serum inorganic phosphate (IP) levels of 2.5 and 1.0 mg/dL after oral administration, during childhood and adulthood, respectively. Treatment included: 1-α hydroxyl vitamin D_3 of 0.05 to 0.1 micro-grams/kg/day and 1.5 to 2.0 micro-grams/day in children and adults, respectively, and phosphate as PO_4 of 120 to 360 mg/kg/day and 36 to 160 mg/kg/day in children and adults, respectively. Renal function in all patients was normal determined by estimated glomerular filtration rate (GFR) calculated using the original Schwartz equation (72 to 191 mL/min/1.73m^2) and no proteinuria. Renal calcification was observed in 11 out of 19 patients who underwent ultrasonography.

Diagnosis of hypophosphatemic rickets was made based on the findings of hypophosphatemia, renal phosphate wasting, elevated alkaline phosphatase levels, absence of aminoaciduria and hypercalciuria, and radiological evidence of rickets or osteomalacia. Mutations in *PHEX* were confirmed by direct sequence for all participants.

Healthy individuals

Healthy control individuals were recruited to participate in this study to establish a reference range for serum FGF23 levels. For a reference range for adults, 111 healthy individuals (from 21 to 63 years old; 34

male, 77 female) were included (reported previously [14]). For a reference range for children, 55 healthy individuals (from 1 month to 18 years old; 27 male, 28 female) were included.

All participants; patients with XLH and surrogates for children, provided written informed consent, as required by the Institutional Review Board of the Metropolitan Children's Hospital.

Methods

Biochemical analysis of FGF23

All the samples were obtained in the morning and stored at -20°C before analysis. Full-length FGF23 (iFGF23) levels in samples were determined by the sandwich ELISA as previously reported with FGF-23 ELISA kit (Kainos, Japan) [14]. Detection limits of the assay ranged from 3 to 800 pg/mL. Inter-assay error was less than 10 %. If iFGF23 levels exceeded 800 pg/mL, samples were diluted with standard reagent in the kit and reassayed.

When two or more determinations per patient were available, the lowest level was selected as data for use in this study to elucidate the lowest level of serum FGF23 in patients with XLH with abnormalities in *PHEX* that could distinguish from healthy subjects. Serum samples were obtained before the meal and oral phosphate administration. Samples were obtained before initiation of therapy with phosphate in four patients, and during periods of noncompliance over more than six years in two patients. Serum samples were obtained from 15 other patients who were current being treated with phosphate. However, compliance was poor in two of the 15 patients upon reviewing the frequency of prescription refills. Serum iFGF23 levels with and without phosphate therapy were available in three of the six patients who did not take phosphate.

Single oral phosphate load and diet

A single oral phosphate load and diet were evaluated as factors which may alter serum iFGF23 levels. As for a single oral phosphate load, serum samples were obtained prior to then subsequently 30, 60, 90, and 120 minutes after oral phosphate administration in patients with abnormalities in *PHEX*. The phosphate load was administered more than two hours after the patient's last meal. Loading dosages of phosphate were the single therapeutic dose in each patient (30 to 115 and 10 to 40 mg/kg as PO_4 in children and adults, respectively). Serum iFGF23 and IP levels were then determined. Correlation between iFGF23 levels and IP was evaluated. Data were available from 23 loading tests performed in 14 patients with abnormalities in *PHEX* (ages 1 to 36 years).

As for the influence of diet in FGF23, serum samples were obtained prior to and subsequently 60 minutes after breakfast in seven healthy control adults (ages 30 to 49 years). Serum iFGF23 levels were determined. General amount of phosphorus in the typical Japanese breakfast is 200 mg to 500 mg.

Analyses of correlation between severity of XLH and iFGF23 levels

The correlations between iFGF23 levels and severity of XLH were investigated. The severity of XLH was determined by gender, age of onset, existence or nonexistence of bone deformity, The ratio of maximum rate of renal tubular reabsorption of phosphate to glomerular filtration rate ($TmPO_4$/GFR), serum IP levels, serum Alkaline Phosphatase (ALP) levels, therapeutic dose of phosphate (mg/kg/day), and the phosphate dosage which increased serum IP levels by 1.5 mg/dL after the oral administration (mg/kg/dose) compared to prior phosphate therapy. Serum IP levels, serum ALP levels, $TmPO_4$/GFR, and therapeutic dose of phosphate were investigated among three age groups (infancy, childhood, adulthood) separately and across the entire age groups. When two or more determinations of serum IP and ALP levels were available, the lowest level before treatment was selected for analyses. When two or more determinations of $TmPO_4$/GFR were available, all data were included for analyses.

Because phenotypic difference may be influenced by genotype of abnormalities in *PHEX* and by gender, the correlations between iFGF23 levels and severity of XLH were also investigated among the members in the same kindred or the same gender siblings.

Statistical analysis

The reference range for serum iFGF23 level was defined as the level between the 5^{th} and the 95^{th} percentiles of healthy individuals. Comparison of iFGF23 levels for each gender and the existence or nonexistence of bone deformity was analyzed by Mann-Whitney's U test. Correlations between iFGF23 levels and age of onset, $TmPO_4$/GFR, serum IP levels, serum ALP levels, therapeutic dose of phosphate, or phosphate dosage which increased serum IP levels by 1.5 mg/dL after the

oral administration were analyzed by Pearson's correlation coefficient. $P<0.05$ was defined as being statistically significant.

Results

Temporal change in iFGF23 levels in response to single oral phosphate load and diet

No general tendency was observed in iFGF23 levels after breakfast in seven healthy individuals (Fig. 1). iFGF23 levels were increased (>5 pg/mL) in three and decreased (>5 pg/mL) in one of seven individuals and not significantly changed (<5 pg/mL) in the other three individuals (Fig. 1). An increasing trend was shown in iFGF23 levels after oral phosphate administration in patients with abnormalities in *PHEX* (Fig. 2). A representative course of iFGF23 and IP levels is shown in Fig. 2a. The increase in iFGF23 levels was subsequent to an increase in IP levels. All time courses of iFGF23 levels from 23 loading tests derived from 14 patients are shown in Fig. 2b. iFGF23 levels increased by over 18 pg/mL from base line in 14 tests from 10 patients, and did not increase (increment <10 pg/mL) in 9 tests from

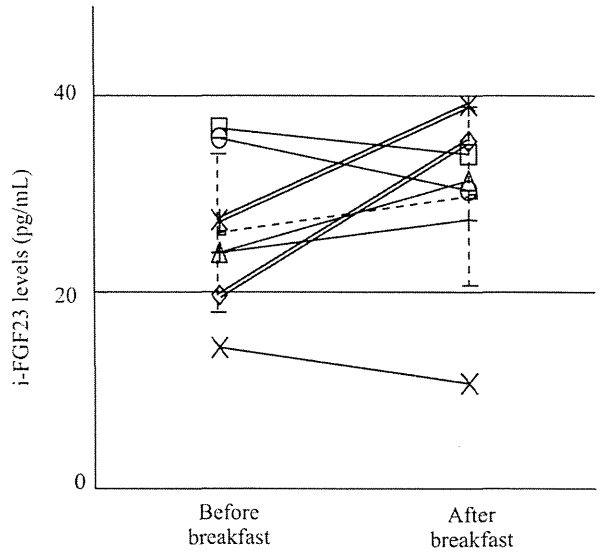

Fig. 1 iFGF23 levels after breakfast
Solid line (—): iFGF23 levels obtained before and after breakfast in seven healthy individuals. Double line (═): Two individuals who showed increase in iFGF23 levels after breakfast (>10 pg/mL). Dashed line (----): Mean and SD of the iFGF23 levels of all healthy individuals. No general tendency was observed in iFGF23 levels after breakfast in healthy individuals.

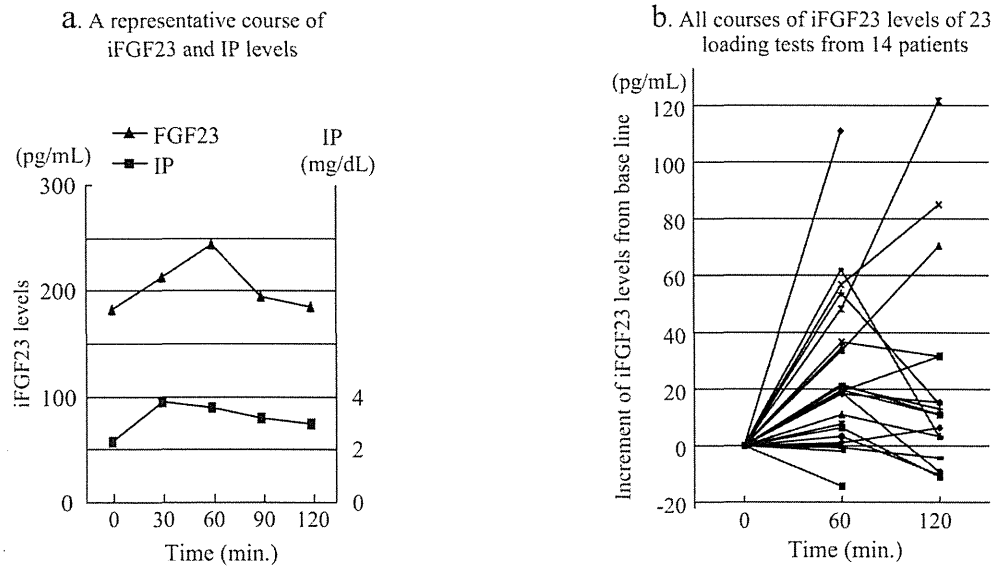

Fig. 2 iFGF23 levels after oral phosphate administration
An increasing trend was shown in iFGF23 levels after oral phosphate administration in patients with abnormalities in *PHEX*. Fig. 2a: A representative course of iFGF23 and IP levels. The increase in iFGF23 levels was subsequent to an increase in IP levels. Fig. 2b: All time courses of iFGF23 levels from 23 tests derived from 14 patients. iFGF23 levels increased over 18 pg/mL (18~111 pg/mL) from baseline in 14 determinations from 10 patients, and did not increase (increment <10 pg/mL) in 9 determinations from 7 patients. Among six patients who had two or more trials of iFGF23 levels changed with phosphate loading, elevation only, reduction only and both elevation and reduction were observed in two, one, and three patients, respectively. There was no relationship between the amount of change in iFGF23 levels and IP levels.

Table 1 Reference range for iFGF23 levels in normal individuals

Age (years old)	n (male : female)	iFGF23 levels (pg/mL)
0 – 5	24 (8 : 16)	12.7 - 45.0
6 – 10	15 (7 : 8)	11.3 - 44.0
11 – 18	16 (12 : 4)	18.3 - 55.6
0 – 18	55 (27 :28)	12.9 - 51.2
21 – 63	111 (34 :77)	11.5 - 48.9

Reference range for serum iFGF23 level was defined as the level between the 5th and the 95th percentiles of healthy individuals

7 patients. Among six patients who had two or more trials of iFGF23 levels changed with phosphate loading, elevation only, reduction only and both elevation and reduction were observed in two, one, and three patients, respectively. There was no relationship between the amount of change in iFGF23 levels and IP levels.

Reference range of iFGF23 in the first two decades of life

The reference ranges (5^{th} and 95^{th} percentiles) for each age group (from 1 month to 5 years old, from 6 to 10 years old, from 11 to 18 years old) are shown in Table 1. There was no significant difference in iFGF23 levels among those three age groups. The reference range across all age groups (from 0 to 18 years old) was from 12.9 to 51.2 pg/mL. The reference range for adults (from 21 to 63 years old) was from 11.5 to 48.9 pg/mL (previously reported) [14]. iFGF23 levels in the first two decades of life were not significantly different from those in adults.

iFGF23 level is higher in the patients with XLH with abnormalities in PHEX than in healthy individuals

Serum iFGF23 levels in XLH with abnormalities in *PHEX* ranged from 40 to 4710 pg/mL before a meal and oral phosphate administration (Fig. 3). Among 14 children (under 20 years old), iFGF23 levels were over 51.2 pg/mL in all patients except one (40.0 pg/mL in one female who was 1 year and 3months old, and >57.8 pg/mL in the other 13 patients). Among 7 adults (20 years and older), iFGF23 levels were over 48.9 pg/mL

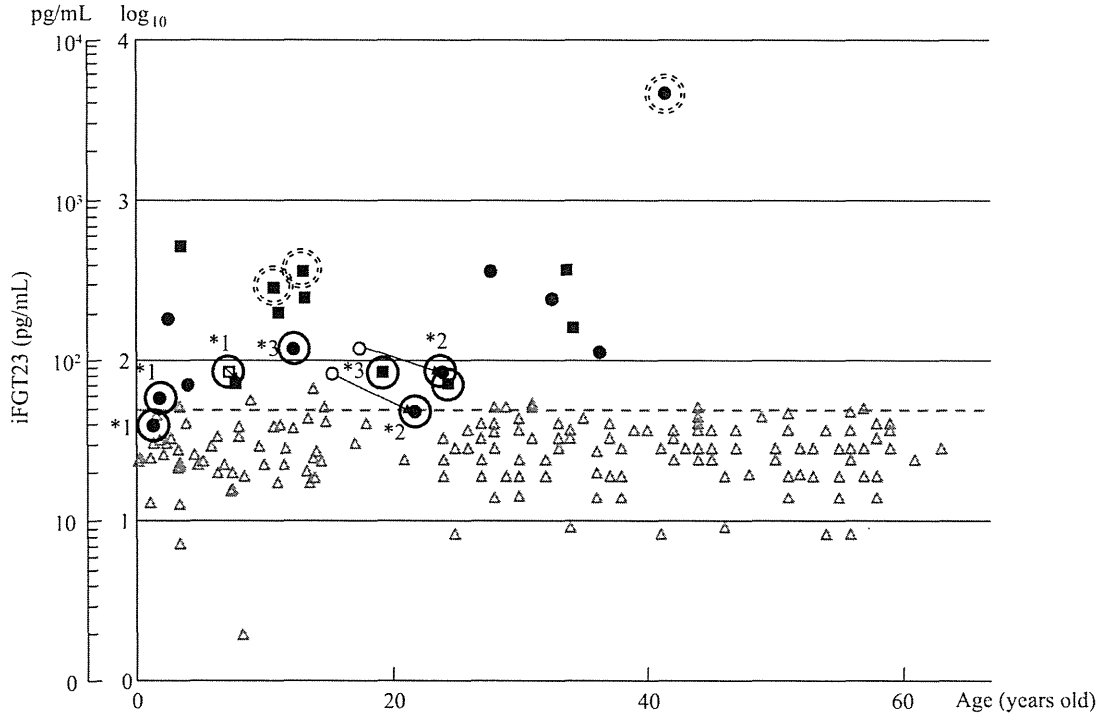

Fig. 3 iFGF23 levels in XLH with abnormalities in *PHEX*
Triangular dots (△): healthy individuals. Broken line (----): upper limit of reference range (95 percentile). Slid square dots (■): male patients with abnormalities in PHEX. Solid circular dots (●): female patients with abnormalities in PHEX. Hollow square dot (□): data obtained before initiation of treatment in male patients with abnormalities in PHEX (□ before → ■ after treatment in the same patient). hollow circular dots (○): data obtained from female patients with abnormalities in PHEX who were noncompliant (○under treatment→●noncompliant in the same patients). Three dots (■●) circled with broken line: A family (mother and her sons) with mutations in PHEX. Dots (●■□) circled with solid line: patients without treatment (*1: before treatment. *2: noncompliance. *3: poor compliance).